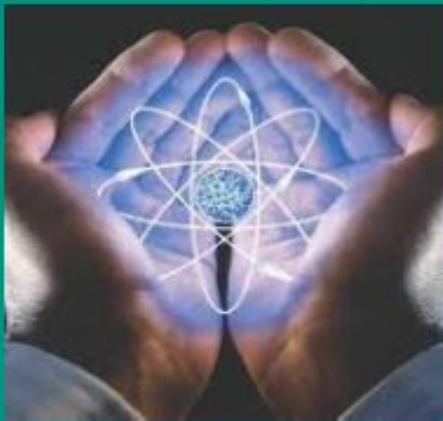


Table Of Content

Journal Cover	2
Author[s] Statement	3
Editorial Team	4
Article information	5
Check this article update (crossmark)	5
Check this article impact	5
Cite this article	5
Title page	6
Article Title	6
Author information	6
Abstract	6
Article content	8

Academia Open



By Universitas Muhammadiyah Sidoarjo

Originality Statement

The author[s] declare that this article is their own work and to the best of their knowledge it contains no materials previously published or written by another person, or substantial proportions of material which have been accepted for the published of any other published materials, except where due acknowledgement is made in the article. Any contribution made to the research by others, with whom author[s] have work, is explicitly acknowledged in the article.

Conflict of Interest Statement

The author[s] declare that this article was conducted in the absence of any commercial or financial relationships that could be construed as a potential conflict of interest.

Copyright Statement

Copyright © Author(s). This article is published under the Creative Commons Attribution (CC BY 4.0) licence. Anyone may reproduce, distribute, translate and create derivative works of this article (for both commercial and non-commercial purposes), subject to full attribution to the original publication and authors. The full terms of this licence may be seen at <http://creativecommons.org/licences/by/4.0/legalcode>

EDITORIAL TEAM

Editor in Chief

Mochammad Tanzil Multazam, Universitas Muhammadiyah Sidoarjo, Indonesia

Managing Editor

Bobur Sobirov, Samarkand Institute of Economics and Service, Uzbekistan

Editors

Fika Megawati, Universitas Muhammadiyah Sidoarjo, Indonesia

Mahardika Darmawan Kusuma Wardana, Universitas Muhammadiyah Sidoarjo, Indonesia

Wiwit Wahyu Wijayanti, Universitas Muhammadiyah Sidoarjo, Indonesia

Farkhod Abdurakhmonov, Silk Road International Tourism University, Uzbekistan

Dr. Hindarto, Universitas Muhammadiyah Sidoarjo, Indonesia

Evi Rinata, Universitas Muhammadiyah Sidoarjo, Indonesia

M Faisal Amir, Universitas Muhammadiyah Sidoarjo, Indonesia

Dr. Hana Catur Wahyuni, Universitas Muhammadiyah Sidoarjo, Indonesia

Complete list of editorial team ([link](#))

Complete list of indexing services for this journal ([link](#))

How to submit to this journal ([link](#))

Article information

Check this article update (crossmark)



Check this article impact (*)



Save this article to Mendeley



(*) Time for indexing process is various, depends on indexing database platform

Dft Computational Study of Organic Inhibitors on the Surface of Iron

Mustafa Jassim Radhi, mustafachem11@gmail.com, (1)

Maisan Education, Iraq

⁽¹⁾ Corresponding author

Abstract

General Background: Corrosion poses a significant global challenge, causing severe economic and structural damage, with approximately 25% of metals produced annually lost due to ongoing degradation. **Specific Background:** Among various mitigation strategies, organic inhibitors are promising for their efficiency and potential environmental compatibility. **Knowledge Gap:** Despite experimental evidence of indoline-2,3-dione derivatives as effective inhibitors, detailed quantum-level insights into their inhibition mechanisms remain limited. **Aims:** This study employs density functional theory (DFT) to evaluate the electronic and chemical interaction parameters of these derivatives and compare predicted performances with experimental data. **Results:** Calculations using Gaussian09 (B3LYP/6-31++G(d,p)) and G311-6/LYP3B basis sets revealed that 5-chloro-1-(2-(N,N-dimethylamino)ethyl)indoline-2,3-dione exhibits superior inhibition efficiency, characterized by a low energy gap (3.314 eV), high inhibitor-metal interaction energy ($\Delta\Psi$), enhanced ductility, and favorable EB-D exchange energy. Mulliken charge distribution and electrostatic potential maps confirmed strong nucleophilic and electrophilic sites, supporting a chemisorption-driven mechanism. **Novelty:** This is the first comprehensive DFT-based analysis linking multiple electronic properties to experimental inhibition data for indoline derivatives. **Implications:** The findings provide predictive guidelines for designing targeted, environmentally friendly corrosion inhibitors for acidic industrial environments, particularly in hydrochloric acid and hydrogen sulfate processing.

Highlights:

- Demonstrates superior inhibition efficiency of specific indoline derivative.
- Links quantum parameters directly to experimental performance.
- Supports eco-friendly corrosion inhibitor design for acidic environments.

Keywords: Corrosion Inhibition, Density Functional Theory, Indoline Derivatives, Quantum Parameters, Chemisorption

Published date: 2025-08-12 00:00:00

Introduction

The development and exploitation of minerals in all fields drives economic progress and prosperity in our current era, as we need them for transportation, construction, and other purposes.[1], [2]

Although metals are distinguished from other materials by their distinctive properties, such as high tensile strength, good flexibility, and electrical conductivity, they have drawbacks, such as their instability when exposed to air, water, and acidic solutions (hydrochloric acid and hydrogen sulfate). They are among the materials most susceptible to corrosion, a dangerous and irreversible natural phenomenon that does not exempt any material from damage or wear.[3]

Most people know that iron rust is the only form of corrosion, as if iron were the only metal capable of exhibiting this phenomenon. However, all metals suffer from it, such as aluminum, metal alloys such as carbon steel (XC70), and ceramics.[4]

Scientists define corrosion as a complex phenomenon that has been scientifically studied since 1830 in all fields, including physics and electrochemistry. This study relies on the mechanical properties of metals .[2]

Corrosion has become a problem that hinders development and a worrying phenomenon due to the enormous damage and losses it causes. Each year, approximately a quarter of the metals produced globally are lost due to the worsening and ongoing corrosion process. This causes enormous losses to the global economy, exceeding expectations and estimated at billions annually. In the United States alone, losses were estimated at approximately \$126 billion in 1982, a significant sum. [5] It also sometimes causes sudden stops in pumping and export operations in factories, resulting in the loss of long working hours. More importantly, corrosion is the leading cause of human casualties, as evidenced by numerous daily accidents, such as water heater explosions, building collapses, transportation accidents, plane crashes, ship sinkings, and bridge collapses, such as the collapse of the Riyadh-Dammam Expressway Bridge on December 19, 2013. The Saudi Ministry of Transport announced, according to Al-Riyadh newspaper, that the cause of the collapse was iron corrosion.[6] Diseases and epidemics resulting either from the leakage of toxic substances from underground pipes into plants and water, and thus to humans, or from the presence of rust in water, all lead to the death of living organisms and cause significant environmental damage if we do not seek to prevent or mitigate them in some way.[7], [8] However, understanding the cause of this problem and how it occurs is sufficient to help find solutions and prevent it. Among the scientific solutions for corrosion protection, we find:

Inhibitors, which are one method that contributes to protecting against the risk of corrosion and its damage. Their types, method of action, and degree of danger vary. Some cause environmental damage over time due to their toxicity, while others maintain their toxicity, such as organic inhibitors, which have proven their inhibitory efficiency in many cases.[7]

Computational Methods

All calculations were performed on an Intel® Core™ i7-7700HQ processor at 2.80 GHz and 2.81 GHz. Bond lengths, total energy, and various electronic properties of the molecules, such as dipole moment, energy of the highest occupied molecular orbital (EHOMO), lowest unoccupied molecular orbital (ELUMO), and quantum parameters, were calculated using Gaussian09 using the B3LYP/6-31++G(d,p) basis set and DFT method.

Results and Discussion

A. Structure of the studied inhibitors

In this study, we selected two organic inhibitors using GaussView. We drew the structure of each inhibitor. We summarize the structure of the studied inhibitors in the following table:

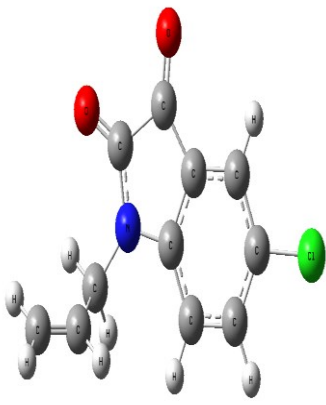
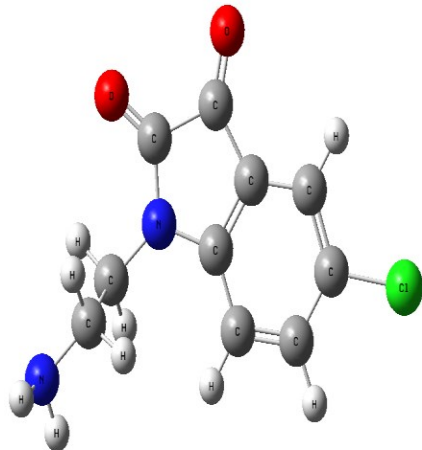
	A1	A2
Structure		
IUPAC nomenclature	1-allyl-5-chloro-indoline-2,3-dione	5-chloro-1-[2-(dimethylamino)ethyl]indoline-2,3-dione
Molecular formula	C ₁₁ H ₁₀ ClNO ₂	C ₁₄ H ₁₇ ClN ₂ O ₂
Molecular size	316 Å°	431.73 Å°
(C _R)corrosion rate at concentration 10 ⁻³ M	0.07	0.04

Table 1. Some properties of corrosion inhibitors (A1, A2)

We note an inverse relationship between inhibitor size and corrosion rate. The second inhibitor, 5-chloro-1-[2-(dimethylamino)ethyl]indoline-2,3-dione, has the largest size and lowest corrosion rate, as demonstrated in most experimental studies .[9]

B. Energy of the Compound

Using a Gaussian program, we draw the structure of each inhibitor molecule. To obtain an improved and more stable structure, we chose the DFT method using the B3LYP/6-311G rule, which is considered one of the best molecular modeling methods.

Minimum energy is a criterion that determines the structure adopted by any compound, i.e., the most stable structure.

The compound 1-allyl-5-chloro-indoline-2,3-dione (A1) went through sixteen stages until it reached its minimum energy, which was found to be: -1089.34635940 AU

AU, while the compound 5-chloro-1-[2-(dimethylamino)ethyl]indoline-2,3-dione (A2) went through sixteen stages until it reached its minimum energy, which was found to be: -1106.62137776 AU.

The structures below were confirmed to be minimal through the frequency values of the infrared spectrum, where we observed the absence of a fictitious (negativity) frequency[10], as can be seen from the infrared (IR) curves shown in Figures (1,2).

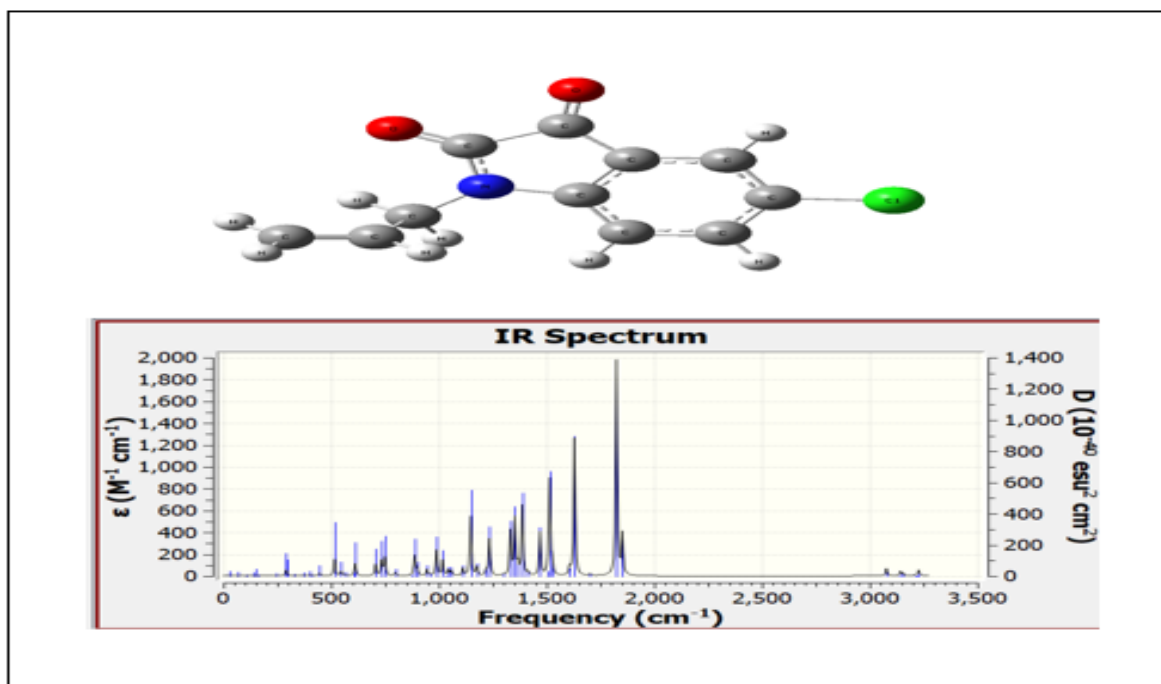


Figure 1. IR spectrum of first inhibitor 1-allyl-5-chloro-indoline-2,3-dione (A1)

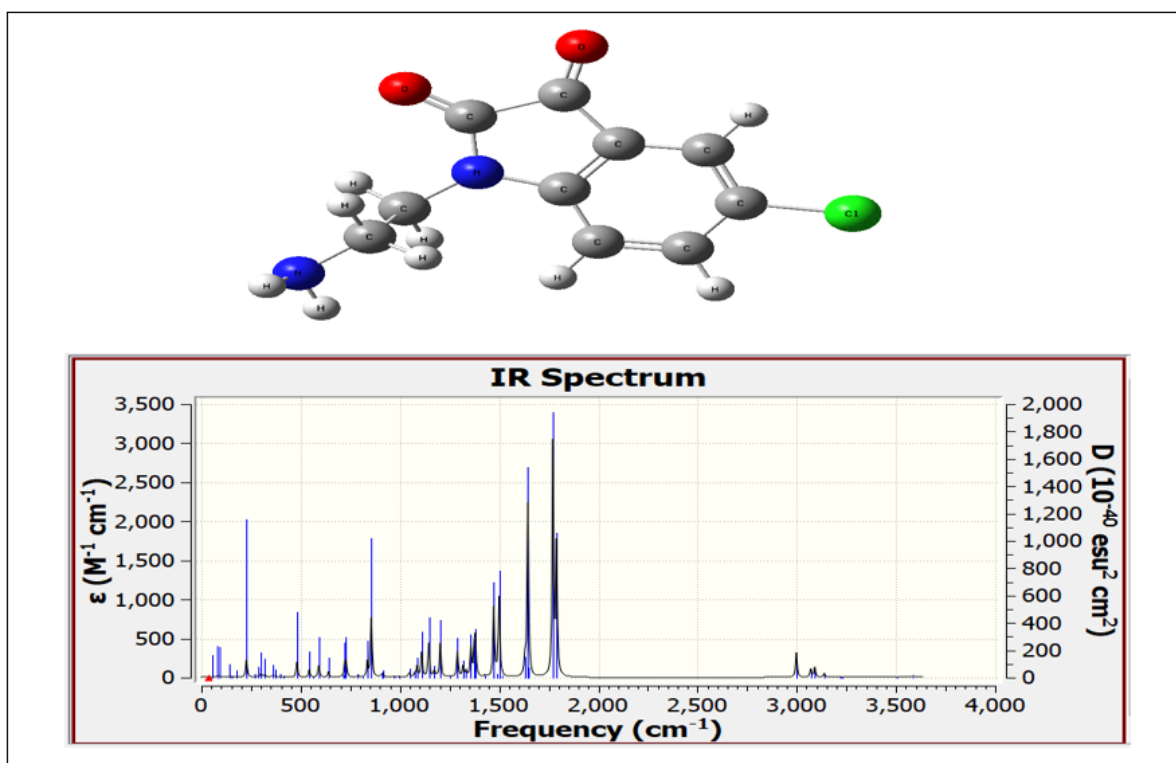


Figure 2. IR spectrum of second inhibitor 5-chloro-1-[2-(dimethylamino)ethyl]indoline-2,3-dione (A2)

C. Structural Study of Compounds

Using Gaussian 09, we calculated the structural bond lengths, as well as the values of of the compound's atomic charges shown in Table 2-3. The modeling was performed using the DFT/B3LYP/6-311 method.

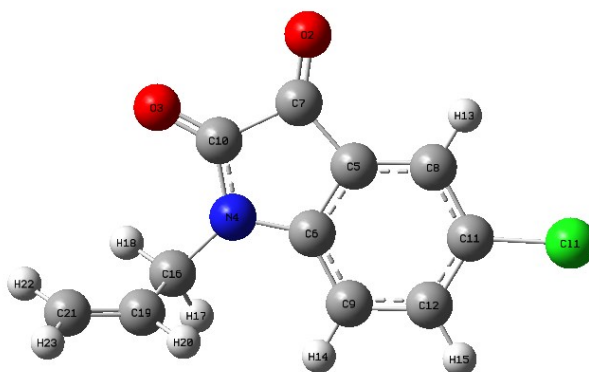
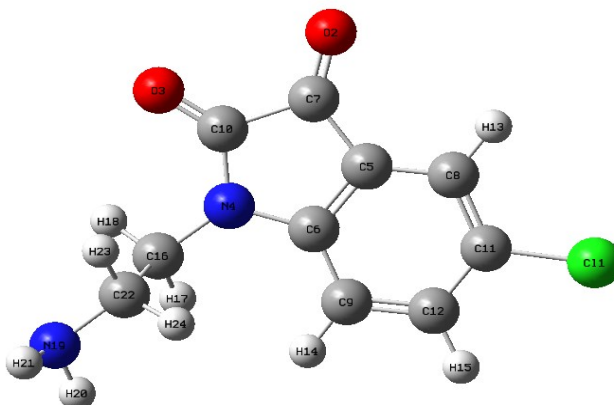


Figure 3. Structural Study of Compounds

values	Length of the bond
1.221	C ₁₀ =O ₃
1.567	C ₁₀ -C ₇
1.372	C ₁₀ -N ₄
1.468	C ₁₅ -N ₄
1.566	C ₇ -C ₁₀
1.095	C ₁₅ -H ₁₇
1.084	C ₈ -H ₁₃
1.769	C-Cl
1.217	C ₇ =O ₂
1.509	C ₁₆ -C ₁₉

Table 2. Values of lengths of the bonds for the inhibitor A1



values	Length of the bond
1.221	C ₁₀ =O ₃
1.567	C ₁₀ -C ₇

1.372	C ₁₀ -N ₄
1.468	C ₂₂ -N ₁₉
1.399	C ₁₁ -C ₁₂
1.100	C ₂₂ -H ₂₄
1.084	C ₁₂ -H ₁₅
1.769	C-Cl
1.217	C ₇ =O ₂
1.461	C ₁₄ -N ₄
1.535	C ₁₆ -C ₂₂

Table 3. Values of lengths of the bonds for the inhibitor A2

1. The lengths of the bonds

Observing the bond lengths, we note that the C-Cl bond is the longest in all inhibitors compared to the other bond lengths, and its value is almost identical across all inhibitors (approximately 1.769 Å). This is due to the difference in electronegativity between the two atoms, as also shown in the Millikan charge value tables 5 ,6 .

The carbonyl bond is almost identical in both inhibitors due to the strong double bond between carbon and oxygen. The C₁₆-C₁₉ bond in the first compound, which contains an allyl group, is shorter (1.509 Å), while C₁₆-C₂₂ bond in the second compound, which contains a substituted amine group, it is longer (1.535 Å) due to the effect of the electron-donating amino group, which weakens the C-N double bond.

2. Frontier orbital energy and general criteria for inhibitor reactivity

Calculating the frontier orbital energy and all derived criteria (quantum parameters) is of critical importance in determining and comparing the efficiency and effectiveness of an inhibitor.[11]

Energy (ev)	(A1) 1-allyl-5-chloro-indoline- 2,3-dione	(A2) 5-chloro-1-[2- (dimethylamino)ethyl]indoline- 2,3-dione
homo	-6.645	-6.603
lumo	-3.3	-3.29
(I)	6.645	6.603
(A)	3.3	3.29
(X) Electronegativity	4.972	4.946
(η) Global Hardness	1.673	1.657
(ΔN) Number of Transferred Electrons	5.702	5.648
(μ) Dipole Moment	-4.972	-4.946
(ω) Electrophilicity Index	0.028	0.027
(E _{gap})	3.346	3.314

($\Delta\Psi$) Metal Interaction Energy	19.436	19.255
(E_{B-D}) Back -donation	-0.418	-0.414
(σ) Global Softness	442.642	446.931

Table 4. Values of quantum parameters for the inhibitors studied

Following the previous table 4, we find:

The second inhibitor (A2), 5-chloro-1-[2-(dimethylamino)ethyl]indoline-2,3-dione, has the lowest energy gap (3.314 eV) value, resulting in the largest number of electrons transferred from the inhibitor to the metal, as shown in the table 4. Therefore, this inhibitor is considered the best and most effective, followed closely by the first inhibitor (A1), 1-allyl-5-chloro-indoline-2,3-dione. We find that it has the largest energy gap value, estimated at (3.346 eV), resulting in the smallest number of transferred electrons, making it the least efficient and least effective. This is what the table illustrates and is consistent with the experimental study[9].

The number of transferred electrons (ΔN) expresses the ability of a compound or inhibitor to gain or donate electrons to or from a metal. If it is $\Delta N > 0$, this means that the compound is donating electrons to the metal, and vice versa if it is $\Delta N < 0$ [12]. From the values in the table, we note that the values of transferred electrons are positive for two inhibitors,, in the following order: $A1 > A2$, indicating the transfer of electrons from the inhibitor to the metal.

We note that all chemical potential (μ) values are negative, indicating the stability of the studied inhibitors, which is related to the electrophilicity value (ω)[13]. We find that the first inhibitor has the lowest value at (-4.972 eV) and the highest value at ω (0.028 eV), indicating an electrophilic tendency. Meanwhile, the second inhibitor has the highest value at μ (-4.946 eV), making it the least stable, and the lowest value at ω (0.027 eV), indicating a nucleophilic tendency.

For the total energy exchange E_{B-D} , the more negative its values, the more energetically favorable the inhibitor is. From the table, we find that all its values are negative for all inhibitors. This criterion is related to the value of η (hardness)[14]. The best inhibitor, which is the second, has the lowest value for (η) hardness (1.657 eV) and the highest value in E_{B-D} (-0.414eV), making it the least stable and therefore the most active and reactive. The opposite is true for the first least efficient inhibitor, which has the highest value for hardness (1.673eV), and therefore it is the most stable inhibitor, making it E_{B-D} (-0.418 eV) and therefore the lowest value least active and reactive.

The second inhibitor also has a high (σ) Global Softness (446.931eV), which enhances its flexibility and makes it more able to interact with the metal surface.

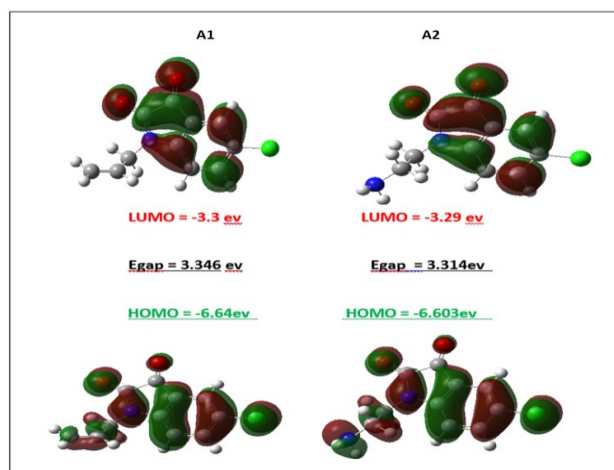


Figure 3. HOMO , LUMO orbitals and E_{gap} of A1 and A2

3. Electrostatic Potential (ESP)

Chemical activity can generally be viewed as the ability of chemical compounds to react with each other to form new chemical compounds. Here, we will infer the chemical activity of a molecule and which areas on its surface will be most active and willing to react with other molecules. We will learn about chemical activity here using an electrostatic density map .

Electrostatic maps, also known as electrostatic energy maps or electrostatic surfaces, illustrate the charge distributions of molecules in three dimensions. They enable us to visualize the charge distributions of molecules and the properties of the charge associated with molecules. They also allow us to visualize the size and shape of molecules in organic chemistry[15], [16]. These maps are very useful in predicting the behavior of molecules, especially complex ones.

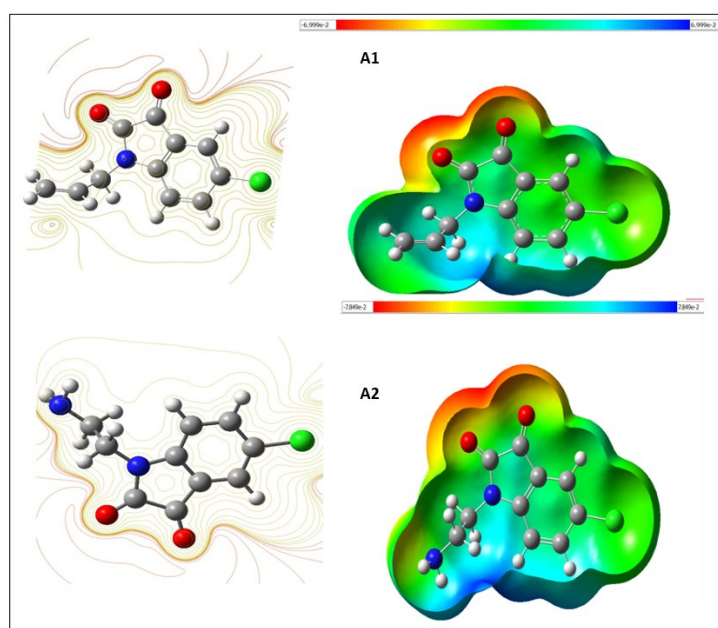


Figure 4. Electrostatics potential (ESP) of A1 and A2

The negative potential regions are electron-rich regions with high electron density. They appear in yellow and red, clearly visible in the oxygen atom, i.e., the heteroatoms in this inhibitor, in all electrostatic maps, as they have a high propensity for nucleophilic attack. These conclusions are reinforced by the Millikan charge values shown in the following tables 5, 6, where they have larger negative values compared to the rest of the atoms.

The positive potential regions are electron-poor regions, ranging in blue from dark to cool. Therefore, these sites represent all the hydrogen atoms (H) in each inhibitor, especially those bonded to N, which appear clearly in dark blue. This is due to the difference in electronegativity between them, which transforms them into electrophilic sites and makes them more susceptible to nucleophilic attack[16]. This is consistent with the Millikan charge values shown in the following tables 5.6 .The regions highlighted in green often represent neutral regions.

4. Charge of atoms using the Millikan method

The Millikan method is one of the most important and widely used methods for calculating charge. It aims to monitor the distribution of negative and positive charges within a compound and the density of electron affinities between atoms, which helps predict nucleophilic and electrophilic sites within the compound[17].

The results and values of the charge of atoms using the Millikan method are closely related to the properties of bonds and angles within the chemical compound, as well as the distribution of electrostatic maps.

label	atom	charge
1	Cl	0.147373
2	O	-0.460778
3	O	-0.501727
4	N	-0.810036
5	C	-0.038864
6	C	0.39232
7	C	0.360797
8	C	-0.154036
9	C	-0.189295
10	C	0.68084
11	C	-0.344127
12	C	-0.135386
13	H	0.249093
14	H	0.240917
15	H	0.249827
16	C	-0.264451
17	H	0.251511
18	H	0.247947
19	C	-0.162533
20	H	0.212356
22	C	-0.380655
23	H	0.202063

Table 4. Millikan Atomic Charges for Each Atom in the Compound as Calculated Using Gaussian 09W.

The Millikan charge values are obtained directly at the ports after using the calculation program Gaussian 09W.

The results obtained based on this are recorded in the following tables and figures:

label	atom	charge
1	Cl	0.267415
2	O	-0.506857
3	O	-0.466419
4	N	-0.07838
5	C	0.266952
6	C	-0.770585
7	C	0.263226
8	C	0.250756
9	C	0.188222
10	C	0.283814
11	C	-0.166807
12	C	-0.304328
13	H	0.175842

14	H	0.164371
15	H	0.178238
16	C	-0.309168
17	H	0.197258
18	H	0.199401
19	N	-0.532382
20	H	0.309864
21	H	0.332296
22	C	-0.312838
23	H	0.213295
24	H	0.156816

Table 5. Millikan charge values of inhibitor A2

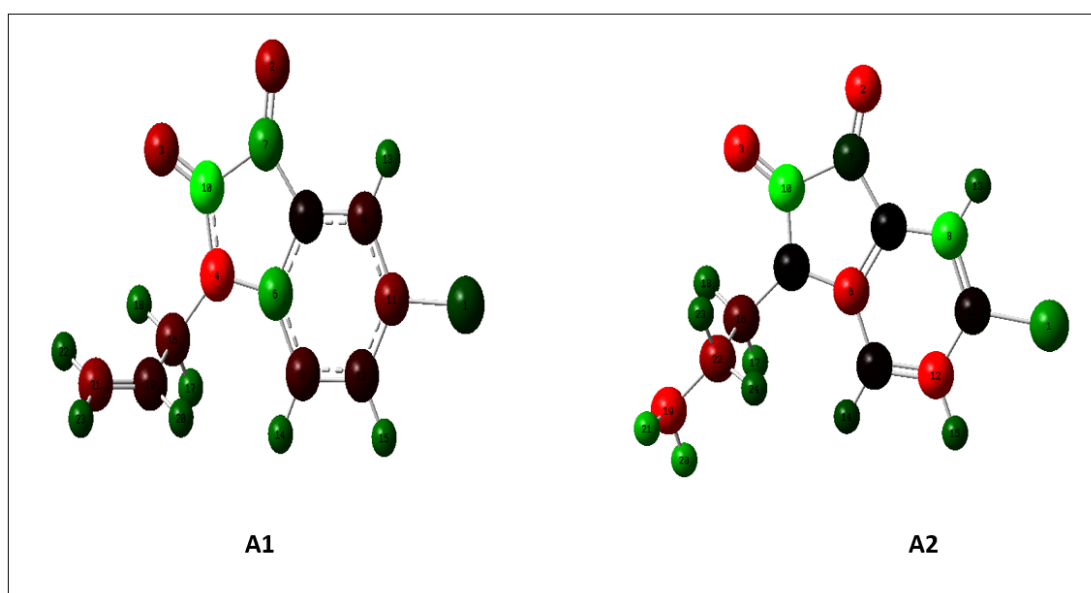


Figure 5. Millikan atoms charges of inhibitors A1 and A2

All compounds are uncharged, meaning their overall charge is zero.

All hydrogen atoms are positive in all inhibitors.

The oxygen (O) and nitrogen (N) atoms in the common core of the heterogeneous inhibitors are negatively charged, thus forming regions susceptible to electrophilic influence.

The carbon atom (C7) has a positive charge in all compounds because it is subject to inductive pull effects. It is an electron-poor region, enhancing its electrophilicity and making it susceptible to the nucleophilic effect. Its highest value is in compound (A1) (0.360797), which is more susceptible to the inductive effect due to the symmetry of the compound, which contains the two oxygen (O) atoms on either side of the carbon (C7) atom. Therefore, it is the most electron-loving site in the three inhibitors.

Through what has been studied of the criteria specific to each atom in the ternary inhibitors, we can say that the heterogeneous atoms of the inhibitors, such as oxygen atoms, have a greater rate of dependence on the nucleophilicity of the inhibitors, which allows us to predict the mechanism of chemical adsorption

between the inhibitor with its nucleophilic sites and the metal surface with the empty d orbitals, as well as the benzene ring through the T electron pair and the mesomeric action in it, as well as through its planar structure, which greatly helps to enhance the bonding and increase the adhesion of the inhibitor to the metal surface, which makes the inhibitory activity excellent

Conclusion

Based on the quantum chemical parameters of both inhibitors, the following conclusions can be drawn:

Both inhibitors exhibit good quantum corrosion inhibition properties. The very high HOMO energies and low energy gaps (gap: 3.34 eV for the first inhibitor and 3.31 eV for the second) indicate a good ability to donate electrons and interact with the metal surface, which is critical for adsorption and inhibition efficiency. The second inhibitor exhibits slightly better reactivity and flexibility, featuring a lower energy gap (3.32 eV vs. 3.34 eV), slightly better ductility (σ : 446.93 vs. 442.64), and lower hardness (η : 1.65 vs. 1.67), indicating its ability to adapt and interact more easily with the metal surface.

Other parameters, such as electronegativity (X), dipole moment (μ), and electron affinity index (ω), are highly similar between the two compounds, indicating similar electron distribution and adsorption behavior. The high electron exchange coefficient ($\Delta\Psi$) values of both inhibitors (greater than 19) indicate their strong ability to transfer electrons to the metal surface, enhancing their inhibition efficiency.

Overall, both compounds are promising corrosion inhibitors, and the second inhibitor is expected to achieve moderate performance improvements due to its lower energy gap and increased digital flexibility. These theoretical results are consistent with experimental studies showing that the second inhibitor is more efficient than the first.

References

- [1] M. Touil, N. Hajjaji, D. Sundholm, and H. Rabaâ, "Computational Studies of the Corrosion-Inhibition Efficiency of Iron by Triazole Surfactants," *International Journal of Quantum Chemistry*, vol. 113, no. 9, pp. 2252–2263, 2013, doi: 10.1002/qua.24310.
- [2] V. S. Litvinenko, "Correction to: Digital Economy as a Factor in the Technological Development of the Mineral Sector," *Natural Resources Research*, vol. 29, no. 5, p. 3413, 2020, doi: 10.1007/s11053-020-09716-1.
- [3] V. S. Raja, "Grand Challenges in Metal Corrosion and Protection Research," *Frontiers in Metals and Alloys*, vol. 1, 2022, doi: 10.3389/ftmal.2022.894181.
- [4] J. C. Gomez-Vidal, "Corrosion Resistance of MCrAlX Coatings in a Molten Chloride for Thermal Storage in Concentrating Solar Power Applications," *npj Materials Degradation*, vol. 1, no. 1, pp. 1–8, 2017, doi: 10.1038/s41529-017-0012-3.
- [5] S. Jung and E. J. Biddinger, "Electrocatalytic Upgrading of Furfural to Produce Biofuels and Fine Chemicals: Synergistic Effects Between Cu Electrocatalysts and Electrolytes," *ECS Meeting Abstracts*, vol. MA2016-01, no. 38, pp. 1935–1935, 2016, doi: 10.1149/ma2016-01/38/1935.
- [6] A. Menga, T. Kanstad, D. Cantero, L. Bathen, K. Hornbostel, and A. Klausen, "Corrosion-Induced Damages and Failures of Post-Tensioned Bridges: A Literature Review," *Structural Concrete*, vol. 24, no. 1, pp. 176–191, 2023, doi: 10.1002/suco.202200297.
- [7] W. Lestari, "Pengaruh Pelayanan Promosi dan Syariah Terhadap Minat Nasabah dalam Memilih Asuransi Syariah (Studi pada PT Asuransi Takaful Keluarga Cabang Palembang)," *Jurnal Chemical Information and Modeling*, vol. 2, no. 1, pp. 15–22, 2015.
- [8] H. M. Hussein Farh, M. E. A. Ben Seghier, R. Taiwo, and T. Zayed, "Analysis and Ranking of Corrosion Causes for Water Pipelines: A Critical Review," *npj Clean Water*, vol. 6, no. 1, pp. 1–19, 2023, doi: 10.1038/s41545-023-00275-5.
- [9] Z. Tribak, M. K. Skalli, and O. Senhaji, "Comparative Studies on the Corrosion Inhibition of Three Different Organic Heterocyclic Compounds as Corrosion Inhibitors for Mild Steel in Hydrochloric Acid," *Journal of the Mexican Chemical Society*, vol. 64, no. 4, pp. 383–392, 2020, doi: 10.29356/jmcs.v64i4.1247.

- [10] V. Luzhkov and A. Warshel, "Microscopic Models for Quantum Mechanical Calculations of Chemical Processes in Solutions: LD/AMPAC and SCAAS/AMPAC Calculations of Solvation Energies," *Journal of Computational Chemistry*, vol. 13, no. 2, pp. 199–213, 1992, doi: 10.1002/jcc.540130212.
- [11] G. Gece and S. Bilgiç, "A Theoretical Study of Some Hydroxamic Acids as Corrosion Inhibitors for Carbon Steel," *Corrosion Science*, vol. 52, no. 10, pp. 3435–3440, 2010, doi: 10.1016/j.corsci.2010.06.005.
- [12] M. Murmu, N. C. Murmu, M. Ghosh, and P. Banerjee, "Density Functional Theory, Monte Carlo Simulation and Non-Covalent Interaction Study for Exploring the Adsorption and Corrosion Inhibiting Property of Double Azomethine Functionalised Organic Molecules," *Journal of Adhesion Science and Technology*, vol. 36, no. 23–24, pp. 2513–2534, 2022, doi: 10.1080/01694243.2022.2057104.
- [13] Ş. Erdoğan, Z. S. Safi, S. Kaya, D. Ö. Işın, L. Guo, and C. Kaya, "A Computational Study on Corrosion Inhibition Performances of Novel Quinoline Derivatives Against the Corrosion of Iron," *Journal of Molecular Structure*, vol. 1134, pp. 62–71, 2017, doi: 10.1016/j.molstruc.2017.01.037.
- [14] U. I. Shehu and B. Usman, "Corrosion Inhibition of Iron Using Silicate Base Molecules: A Computational Study," *Advanced Journal of Chemistry – Section A*, vol. 6, no. 4, pp. 399–408, 2023, doi: 10.22034/ajca.2023.399262.1375.
- [15] S. Grimme, "Molecular Electrostatic Potentials: Concepts and Applications," *Zeitschrift für Physikalische Chemie*, vol. 205, no. 1, pp. 135–153, 1998, doi: 10.1524/zpch.1998.205.part_1.136b.
- [16] E. Scrocco and J. Tomasi, "The Electrostatic Molecular Potential as a Tool for the Interpretation of Molecular Properties," in *New Concepts II*, Berlin, Germany: Springer, 2007, pp. 95–170, doi: 10.1007/3-540-06399-4_6.
- [17] Y. Gu and D. Li, "Measurements of the Electric Charge and Surface Potential on Small Aqueous Drops in the Air by Applying the Millikan Method," *Colloids and Surfaces A: Physicochemical and Engineering Aspects*, vol. 137, no. 1–3, pp. 243–256, 1998, doi: 10.1016/S0927-7757(97)00366-X.